Available online at www.sciencedirect.com

ScienceDirect

Geochimica et Cosmochimica Acta 237 (2018) 18–31

Geochimica et Cosmochimica Acta

www.elsevier.com/locate/gca

Large carbon isotope variability during methanogenesis under alkaline conditions

Hannah M. Miller [a,*], Nabil Chaudhry [a], Mark E. Conrad [b], Markus Bill [b], Sebastian H. Kopf [a], Alexis S. Templeton [a,*]

[a] Department of Geological Sciences, UCB 399, University of Colorado, Boulder, CO 80309, USA
[b] Earth Sciences Division, MS 70A-4418, E.O. Lawrence Berkeley National Laboratory, Berkeley, CA 94720, USA

Received 17 October 2017; accepted in revised form 6 June 2018; available online 27 June 2018

Abstract

High carbon isotope values ($\delta^{13}C_{CH4} > -40‰$) have widely been used as evidence that methane in alkaline rock-hosted fluids was formed abiotically, particularly in serpentinizing systems. However, isotope fractionation during microbial methanogenesis is relatively understudied at high pH. We isolated a hydrogenotrophic *Methanobacterium* sp. from hyperalkaline subsurface fluids in the Samail ophiolite to assess how carbon and hydrogen isotope values of CH_4 varied depending upon pH and carbonate mineral source ($NaHCO_3$ or $CaCO_3$). The hydrogen isotope fractionation $\alpha_{H20/CH4}$ (1.46–1.66) did not vary across pH. In contrast, the expressed carbon isotope fractionation, $\alpha_{CO2/CH4}$, ranged from 1.028 to 1.089. Carbon isotope fractionation increased with pH, reaching a maximum ^{13}C depletion of −85‰. However, the ^{13}C depletion significantly diminished at pH ≥ 9 for $CaCO_3$-amended experiments, generating $\delta^{13}C_{CH4}$ as high as −28‰. To evaluate the large variability in $\delta^{13}C_{CH4}$, we developed a steady-state model to assess how the rates of carbonate dissolution, cellular uptake of CO_2 and irreversible CH_4 production can affect the net isotope fractionation during methanogenesis. *Methanobacterium* sp. can produce highly depleted $\delta^{13}C_{CH4}$ in simulated alkaline serpentinizing fluids when dissolved inorganic carbon levels are high and methanogenesis rates are slow. However, small carbon isotope fractionation occurs when rates of carbonate dissolution are slower than cellular uptake, leading to relatively high $\delta^{13}C_{CH4}$ values (>∼−35‰) that are traditionally interpreted to be purely "abiotic". Thus, microbial CH_4 can be produced in carbon-limited mafic and ultramafic rock-hosted environments on Earth and potentially other planetary bodies, but it may be difficult to isotopically identify biogenic methane when mineral carbonates are the dominant carbon source.

Keywords: Methanogenesis; Carbon isotopes; Ophiolites

1. INTRODUCTION

Hydrogenotrophic methanogenesis, a strictly anaerobic metabolism in which organisms reduce CO_2, formate or CO while utilizing hydrogen, is a commonly predicted metabolism in the shallow subsurface of the Earth. Hydrogenotrophic methanogens have been found inhabiting diverse H_2-rich rock-hosted systems: subsurface basalt aquifers in Idaho (Chapelle et al., 2002), hydrothermal vents (Proskurowski et al., 2006; Takai et al., 2008; Eecke et al., 2012), deep sediments in quartzite-hosted fractures (Moser et al., 2005), and low-temperature continental serpentinizing environments (Barnes et al., 1967; Barnes et al., 1978; Woycheese et al., 2015; Klein et al., 2015; Kohl et al., 2016; Miller et al., 2016; Rempfert et al., 2017). Methanogens living in hard-rock systems may have

* Corresponding authors.
E-mail addresses: hannah.miller2@colostate.edu (H.M. Miller), alexis.templeton@colorado.edu (A.S. Templeton).

https://doi.org/10.1016/j.gca.2018.06.007
0016-7037/

been some of the earliest life forms (Sleep et al., 2004; Nealson et al., 2005; Russell et al., 2010). It is hypothesized that subsurface methanogens may be powered solely by geological processes, independent of products of photosynthesis, utilizing H_2 generated through geological water/rock and/or radiolysis reactions to reduce dissolved CO_2 (Nealson et al., 2005). Additionally, Mars, Europa, and/or Enceladus could support hydrogenotrophic methanogenesis fueled by H_2-generating water/rock reactions (Oze, 2005; Nealson et al., 2005; Blank et al., 2009; Ehlmann et al., 2010; Kral et al., 2014; Glein et al., 2015).

Low-temperature continental serpentinizing systems, as both analogs for planetary bodies and potential early Earth environments, provide an important, yet understudied, methanogen habitat. Hydrogenotrophic methanogens, and specifically *Methanobacterium* sp., have been detected in fluids in the Del Puerto ophiolite, the Cedars, the Zambales ophiolite and the Samail ophiolite (Blank et al., 2009; Suzuki et al., 2014; Woycheese et al., 2015; Miller et al., 2016). However, the alkaline to hyperalkaline serpentinizing fluids (pH > 9–12) limit the bioavailable form of $CO_{2\,(aq)}$ necessary for the biochemical conversion of CO_2 to CH_4 (Madigan, 2012; Suzuki et al., 2014). Water/rock reactions during serpentinization further deprive fluids of carbon by releasing Ca^{2+} or Mg^{2+} ions into the fluids, causing carbonate minerals to precipitate (Barnes et al., 1967). These carbonates can be used for carbon fixation under hyperalkaline conditions, as shown by H_2-utilizing Betaproteobacteria *Serpentinomonas* (Suzuki et al., 2014). Calcite and magnesite can also be utilized for neutrophilic methanogenesis by diverse methanogens such as *Methanothermobacter wolfeii*, *Methanosarcina barkeri*, *Methanobacterium formicum* and *Methanoccocus maripaludus* (Kral et al., 2014). The release of inorganic carbon from carbonate should occur whenever a system is locally perturbed from equilibrium with $CaCO_3$, which could occur due to biological uptake of dissolved inorganic carbon, or changes in pH due to release of protons or organic acids. However, whether methanogens actively solubilize carbonate to produce methane under alkaline and hyperalkaline conditions has not been extensively tested.

Serpentinizing environments commonly contain millimolar to micromolar concentrations of dissolved methane. This methane is typically inferred to be of abiotic origin based on the isotopic composition, distributions of higher hydrocarbons, and/or geological setting (Barnes et al., 1967; Barnes et al., 1978; Abrajano et al., 1990; Lollar et al., 1993; Proskurowski et al., 2006; Etiope et al., 2011; Etiope and Sherwood Lollar, 2013; Morrill et al., 2013). CH_4 from hyperalkaline serpentinizing fluids in the Philippines, Canada, Turkey, Oman, Lost City hydrothermal field and New Zealand has $\delta^{13}C_{CH4}$ values ranging from approximately −35 to −5‰, and the CH_4 is considered to originate from abiotic reduction of carbon under reducing conditions (Abrajano et al., 1990; Proskurowski et al., 2006; Etiope et al., 2011; Etiope et al., 2011; Etiope and Sherwood Lollar, 2013; Szponar et al., 2013). The abiotic methane hypothesis is also supported by measurements of increasingly negative $\delta^{13}C$ values from C_2 to C_5 alkanes (Proskurowski et al., 2008; Etiope et al., 2011). However, there is an acknowledged partial microbial contribution to the CH_4 in Lost City and the Cedars serpentinizing systems (Proskurowski et al., 2008; Bradley and Summons, 2010; Morrill et al., 2013; Kohl et al., 2016) based on ratios of CH_4/C_{2+} (higher chain hydrocarbons) versus $\delta^{13}C_{CH4}$ values.

There is currently debate about the contribution of microbial methane to serpentinizing environments. Microbial production of CH_4 through methanogenesis is considered to produce a unique range of $\delta^{13}C$ and δD CH_4 values (Schoell, 1980; Whiticar, 1999; Valentine et al., 2004; Etiope, 2009; Etiope and Sherwood Lollar, 2013). Microbial CO_2 reduction and acetate fermentation typically generate CH_4 with a $\delta^{13}C$ of −110 to −45‰ and a δD ranging from −375 to −150‰ (Whiticar, 1999; Valentine et al., 2004; Etiope et al., 2013). Miller et al. (2016) measured isotopically enriched $\delta^{13}C_{CH4}$ (−2.4 to 3‰) collected from subsurface fluids in an actively serpentinizing aquifer in the Samail Ophiolite in Oman. Etiope (2016) strongly advocated an abiogenic origin for this methane on the basis of its isotopic composition and geologic setting. However, Miller et al. (2017) noted that 16S rRNA sequencing of these fluids reveals the presence of both known methanogens (*Methanobacterium* sp.) and methane oxidizers such as *Methlyococcus* sp.

The carbon and hydrogen isotope values of CH_4 from alkaline conditions, such as soda lakes and subsurface fluids, are understudied (Oremland et al., 1982; Worakit et al., 1986; Kiene et al., 1986; Mathrani et al., 1988; Kotelnikova et al., 1998; Kohl et al., 2016). Additionally, these methanogens isolated from saline, alkaline soda lakes generally utilize methyl groups for catabolism (Kiene et al., 1986), not hydrogen and CO_2-type substrates as would be expected in serpentinizing environments. Recent work by Kohl et al. (2016) examined the isotopic composition of methane produced under hyperalkaline pH by enrichment cultures of unidentified methanogens from the Cedars in California. The $\alpha_{CO2\text{-}CH4}$ varied from 1.068 to 1.078 and there was a maximum $\alpha_{H2O\text{-}CH4}$ of 1.50, falling within the predicted isotope compositions of biogenic methane. However, Kohl et al. (2016) acknowledged that further experiments are needed to understand isotope systematics of microbially-produced CH_4 in serpentinizing environments, which we further address in this study.

This study investigates the carbon and hydrogen isotope fractionation of microbially produced CH_4 over a wide range of pH and carbon availability. *Methanobacterium sp. NSHQ4* was isolated from hyperalkaline H_2 and CH_4 rich fluids at well NSHQ04 in Oman (see Miller et al., 2016) and cultivated in a synthetic medium made to mimic the environment. We designed experiments with *Methanobacterium NSHQ4* enrichment cultures from pHs of ~7–11 and provided bicarbonate ($NaHCO_3$) and carbonate ($CaCO_3$) as respective carbon sources, then measured the $\delta^{13}C$ and δD values of the CH_4 produced. A steady state model was generated to complement and interpret the experimental data. Additionally, we modeled the partial oxidation of the $\delta^{13}C_{CH4}$ produced by methanogenesis at high pH under carbon limitation in our laboratory experiments to assess the effect of subsequent oxidation on the methane isotopic

composition. The goal was to examine whether some of the notably enriched $\delta^{13}C$ CH_4 values observed in serpentinizing systems could be generated through coupled microbial methanogenesis and methane oxidation.

2. METHODS

2.1. Cultivation of alkaliphilic Methanobacterium NSHQ4

In January 2014, a shallow submersible pump was used to collect biomass by filtering fluids (~5–10 L) obtained from 18 m depth in well NSHQ04 in the Tayin block of the Samail Ophiolite in the Sultanate of Oman (for more information, see Miller et al. 2016). The 0.2 μm Sterivex inline filters were then put in a 100 mL sterilized, silica serum vial and filled with site water, which was then capped to maintain the anaerobic site environment. The vials were then amended with hydrogen, carbon sources (headspace CO_2, formate, $NaHCO_3$) and other mineral components (Fe-oxides and carbonate). The goal of adding all these amendments was to stimulate robust methanogen growth with a variety of carbon sources, and then clean up the media to pinpoint specific metabolisms. *Methanobacterium NSHQ4* was sequentially isolated from NSHQ04 fluids through successive transfers into new, sterilized vials, first growing for 6 generations in site water with 80% H_2:20% CO_2, 0.1 mL Fe(III) oxides, 1 mL 100 mM formate, and 1 mL Oman crushed serpentinite rock, then transferred into sterilized DSMZ methanogen medium 141 (Supplementary Tables 1 and 2). Eventually, *Methanobacterium NSHQ4* enrichment cultures grew in a synthetic NSHQ04 medium (16 mM NaCl, 6 mM $CaCl_2$, 0.0013 mM H_4SiO_4, 0.007 mM $MgSO_4 * 7H_2O$, 0.4 K_2SO_4, 0.01 KNO_3, 0.001 NaF, 0.028 NaBr, 4.13 mM cysteine). After numerous dilutions-to-extinction, the culture was dominated by mesophilic long rods that will grow at 40 °C but not at 55 °C. The culture was not pure; microbial community composition of the methanogenic enrichment culture was determined by sequencing DNA extracted cultures with the MoBio PowerSoil kit (see Supplementary Table 1) using the same methods outlined in Miller et al. (2016).

Supplementary data associated with this article can be found, in the online version, at https://doi.org/10.1016/j.gca.2018.06.007.

2.2. Methane production with $NaHCO_3$ or $CaCO_3$ as the C source

Methanogens were grown in 100 mL sterilized, silica serum vials sealed with butyl rubber stoppers. For each experiment, 90 mL of sterilized medium was added and the headspace was purged with 95% N_2: 5% H_2 and was slightly over-pressurized. Cultures were either grown with 10 mM $NaHCO_{3(aq)}$ (Sigma Aldrich, powder $\delta^{13}C_{DIC} = -3.83‰$) or with an excess of $CaCO_{3(s)}$ (Fisher Scientific, powder $\delta^{13}C_{DIC} = -0.10‰$) that did not fully dissolve. In addition, 0.9 mL of trace vitamins and elements for DSMZ medium 141 were added, as well as 1.8 mL of filter sterilized antibiotic mixture containing 5 mg penicillin, 5 mg streptomycin, and 50 μL ampicillin in order to suppress any bacterial activity. pH was measured with a Thermo Scientific Orion PerpHecT ROSS Combination pH Micro Electrode calibrated with reference standards of pH 4, 7, 10, and 11 ± 0.01. The vials were amended with aqueous solutions of dissolved $NaHCO_3$ or a poorly dissolved solution of $CaCO_3$ and then allowed to sit overnight before the pH values were measured. pH was measured by removing ~0.10 mL of fluid from the serum vials and immediately measuring to prevent equilibration with atmospheric CO_2.

For the $CaCO_3$-amended experiments, 9 vials were inoculated at a range of starting pHs (6.5, 7, 8.5, 9.7, 10.12, 10.38, 10.83, 11.51, 11.94). For the $NaHCO_3$-amended experiments, 9 vials at similar pH were also inoculated (see Table 1). A parallel set of control vials were also prepared for each carbon source (9 $NaHCO_3$-amended and 9 $CaCO_3$-amended) to allow for isotopic analysis of DIC pools. In preliminary experiments, we identified that the pH for each individual experiment was sufficiently variable that it would not be possible to average together replicates. Thus, the goal in these final experiments was to initiate a sufficient number of biological and abiotic experiments across the pH range 6.5–12 to identify the full range in carbon isotope variability across these alkaline and hyperalkaline pH.

All methanogenesis experiments were inoculated with 2 mL from a successfully growing culture in an identical medium and incubated for 154 days. Gas phase H_2, CO_2 and CH_4 concentrations were initially monitored daily, then weekly or biweekly once it was evident growth was slow. Headspace CH_4 concentrations in $NaHCO_3$ and $CaCO_3$ cultures were measured over time and sampled for isotopic analysis once ~0.04 mM aqueous CH_4 was produced SI Fig. 1 and Table 1). 5 mL of headspace gas was sampled for isotopic analysis by injecting it into an evacuated 7 mL vial, and then overpressurizing the bottle with an additional 3 mL of He gas. To ensure sampling itself did not result in isotope fractionation, after the headspace gas was pulled into the syringe, it was equilibrated for ~10 s before removing from the serum vial.

2.3. Concentrations and isotopic analysis of H_2 and CH_4

H_2 and CH_4 concentrations in the gases were measured by injection of 500 μL headspace sample into an SRI 8610C gas chromatograph (GC) equipped with a 2 m by 1 mm ID micropacked ShinCarbon ST column with N_2 as the carrier gas. H_2 and CH_4 were quantified by thermal conductivity (TCD), and flame ionization (FID) detectors, respectively against calibrated standard gases. The detection limit was 10 ppm with an analytical error of 5%. H_2 is known to slowly diffuse out of butyl stoppers. This was tested and studied in Miller et al. (2017), with the conclusion that ~1 nmol of H_2 is lost from the vials per day.

Stable isotope analyses were conducted at the Center for Isotope Geochemistry at the Lawrence Berkeley National Laboratory. The hydrogen and carbon isotopic compositions of H_2 and CH_4 were analyzed using a Thermo Scientific GC Trace Gas Ultra interfaced to a combustion system (for carbon, 1030 °C, Ni/Cu/Pt catalyzed) or pyrolysis furnace (for hydrogen, 1450 °C) connected to a Thermo Scientific Delta V Plus Mass Spectrometer (IRMS) (Brass and

Table 1
Observed fractionation factor calculations. Cultures did not produce sufficient CH_4 at high pHs to measure isotopic values of CH_4. All δ values are in ‰ units. *$\delta^{13}C$ CO_2 values are calculated from Mook (50) calculations of isotopic values for carbon speciation as shown in SI Figs. 2 and 3. **pH of experiments at the time of CH_4 extraction from headspace for isotopic analysis. Reproducibility values are provided in Section 2.

Initial pH	**pH when CH_4 extracted from headspace	$\delta^{13}C$ CH_4	δD CH_4	*$\delta^{13}C$ CO_2	$^{13}\alpha_{NaHCO3/CH4}$	$^{13}\alpha_{CO2/CH4}$	$^{2}\alpha_{H2O/CH4}$
HCO_3				δD H_2O	−108	$\delta^{13}C$ HCO_3	−3.83
6.87	6.92	−54.6	−399	−9.5	1.054	1.048	1.485
7.23	7.12	−56.3	−388	−10.2	1.056	1.049	1.458
7.81	7.71	−69.7	−414	−10.7	1.071	1.063	1.522
8.26	8.45	−76.0	−461	−10.9	1.078	1.070	1.656
9.14	9.24	−85.4	−446	−10.9	1.089	1.081	1.611
9.53	9.55	−82.8	−418	−10.9	1.086	1.078	1.533
9.98	10.08	−84.7	−410	−10.9	1.088	1.081	1.513
10.99	10.85						
11.73	11.28						
				Average	1.075	1.067	1.539
$CaCO_3$						$\delta^{13}C$ $CaCO_3$	−0.1
6.87	7.11	−63.3	−398	−6.0	1.061	1.069	1.481
7.08	7.2	−64.3	−394	−6.5	1.062	1.069	1.473
7.75	7.93	−72.9	−441	−7.3	1.071	1.079	1.595
8.59	8.97	−54.7	−409	−7.4	1.050	1.058	1.510
9.15	8.87	−27.6	−410	−7.5	1.021	1.028	1.512
9.66	9.23	−28.0	−431	−7.4	1.021	1.029	1.568
10.21	9.2						
11.12	10.03						
11.85	11.34						
				Average	1.055	1.048	1.523

Röckmann, 2010; Komatsu et al., 2011). Reproducibility of H_2 analyses is ±2.5‰ (1σ), as determined by repeated analyses of a laboratory gas standard. The reproducibility of carbon analyses is ±0.2‰. For hydrogen isotopes of CH_4, the reproducibility is ±5‰.

2.4. Steady state model

The isotopic fractionation modeling was implemented in R (R Development Core Team, 2008), using the following packages: dplyr, ggplot2, tidr, tibble, readxl, and gridExtra. Equations were verified in Mathematica (Wolfram Research, Inc., 2017).

3. RESULTS

3.1. Methane production and isotopic composition across pH

Methane production occurred to a variable extent across the experimental range of pH, with a maximum calculated rate of 0.094 nmols CH_4/L/sec observed between pH 7.5–8 when *Methanobacterium NSHQ4* was grown with $NaHCO_3$ or $CaCO_3$ provided as the sole carbon source (Fig. 1). For the $NaHCO_3$ experiments, the production of >0.04 mM CH_4 required 11–21 days of growth for the lower pH (<9) cultures, and 37–97 days for the pH 9–10 cultures. At high pH (10.99 and 11.73) CH_4 was not detected. For the vials amended with $CaCO_3$, the lower pH cultures (<8) produced >0.04 mM of CH_4 in only 8 days. The vials with a pH > 9 grew more slowly and did not produce >0.04 mM CH_4 until 45–98 days. The $NaHCO_3$ and $CaCO_3$ experiments stopped generating CH_4 once headspace concentrations stabilized at ~0.08 mM, due to H_2 limitation. The initial fluid pH values for the 9 $NaHCO_3$ and 9 $CaCO_3$ vials spanned from 6.87 to 11.73 (Table 1). In general, fluids experienced a slight decrease in pH as methane accumulated.

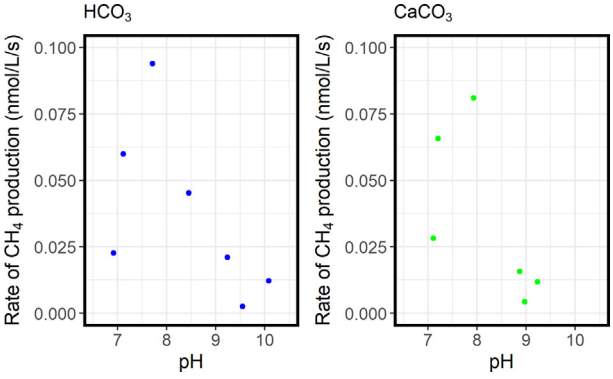

Fig. 1. Maximum rate of CH_4 production (nmol/L/s) versus pH for HCO_3 and $CaCO_3$ experiments. The pH values were measured at the time of sampling headspace gas.

The $\delta^{13}C_{CH4}$ values produced by *Methanobacterium NSHQ4* was measured over the range of pHs (Fig. 2). The $\delta^{13}C_{DIC}$ from $NaHCO_3$-amended experiments is −3.83‰ and $CaCO_3$-amended experiments is −0.10‰. At

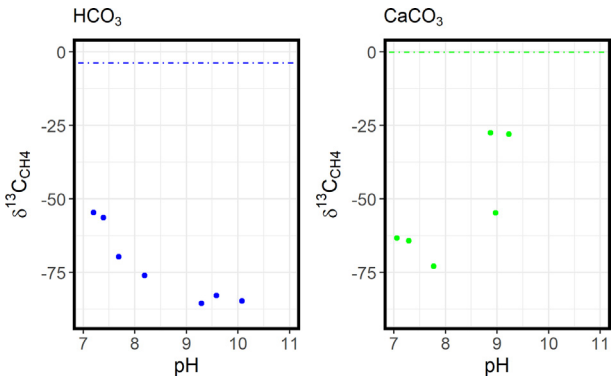

Fig. 2. pH vs $\delta^{13}C$ CH_4 for cultures of Methanobacterium NSHQ4 grown with either HCO_3- (green) or $CaCO_3$ (blue) carbon sources. pH corresponds to the pH of the medium at the time of CH_4 sampling. Dashed blue line shows the initial $\delta^{13}C$ of the $NaHCO_3$ (−3.83‰) and dashed green line shows the initial $\delta^{13}C$ of $CaCO_3$ (−0.10‰). (For interpretation of the references to colour in this figure legend, the reader is referred to the web version of this article.)

higher pHs, the $\delta^{13}C_{CH4}$ becomes more negative, decreasing from −55 to −85‰ in the $NaHCO_3$-fed cultures. From pH 7.11 to 7.93, $CaCO_3$-amended cultures have similar $\delta^{13}C_{CH4}$ values, but at pH ≥ 9, the $\delta^{13}C_{CH4}$ increases to values as high as −28‰. This is in sharp contrast to $\delta^{13}C$ values of −76 to −85‰ in similar pH ranges with $NaHCO_3$ experiments.

The initial δD_{H2O} is −108‰ in NSHQ04 medium and δD_{H2} is −131‰. The δD_{CH4} for culture growing with $CaCO_3$ and $NaHCO_3$ was also measured (Fig. 3). $NaHCO_3$-fed cultures had a tight range of values, δD_{CH4} −399 to −446‰. $CaCO_3$-fed cultures also displayed a similar range of values, δD_{CH4} −394 to −441‰.

3.2. Hydrogen and carbon fractionation factor calculations for $NaHCO_3$ vials

In order to easily compare isotope variations amongst different species of methanogens, we calculated the net fractionation factor both between the accumulated CH_4 and $NaHCO_3$ as well as between CH_4 and CO_2 in the system, assuming CO_2 to be in equilibrium with the practically infinite reservoir of dissolved inorganic carbon from $NaHCO_3$ (total CH_4 produced was <0.08% $NaHCO_3$, SI Fig. 1). The fractionation factors were calculated using the standard equation for open systems (Valentine et al., 2004):

$$\alpha_{x/CH4} = {}^{13}R_x/{}^{13}R_{CH4} = (\delta^{13}C_x + 1000)/(\delta^{13}C_{CH4} + 1000) \quad (1)$$

with $x = HCO_3$ or CO_2. The $NaHCO_3$ substrate was measured as $\delta^{13}C = -3.83‰$. To calculate the corresponding pH-dependent $\delta^{13}C_{CO2}$ values (Table 1), first the concentrations of the carbon species ($H_2CO_{3(aq)}$, HCO_3^-, and CO_3^{2-}) were determined at the pH of each vial, assuming a total of 10 mM DIC in solution (SI Figs. 2 and 3). Carbon speciation was calculated using a pKa_1 of 6.296 and pKa_2 of 10.220 (Benjamin, 2002). The predicted isotope composition of each dissolved carbon species at each pH can be quantitatively calculated at 40 °C (313.15 K) based on the

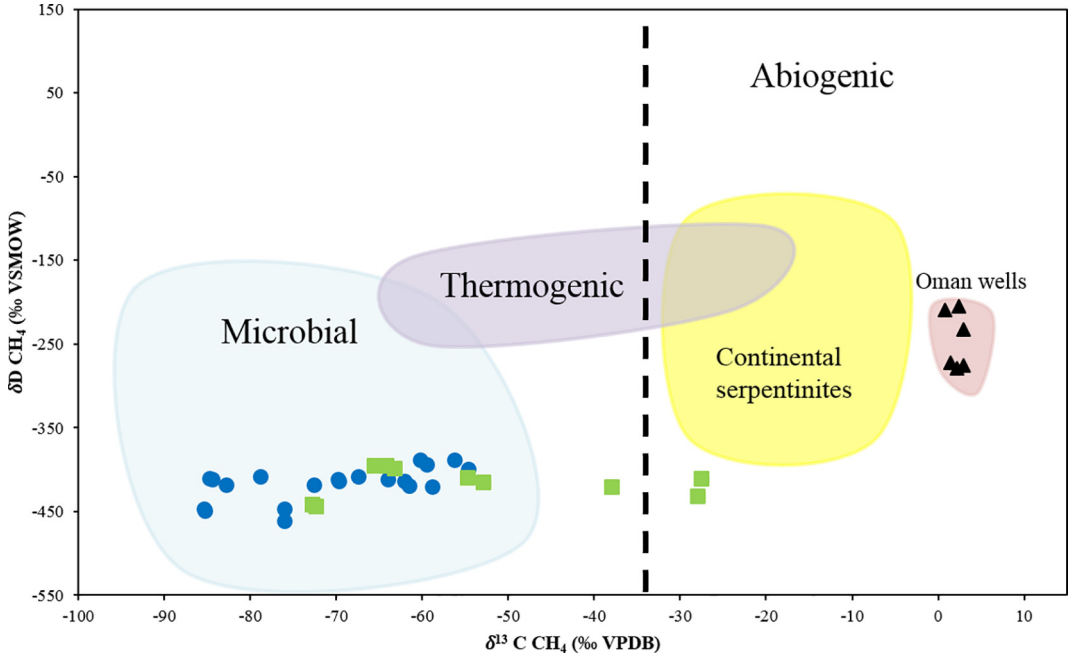

Fig. 3. The δD and $\delta^{13}C$ values of CH_4 show CH_4 isotope values for *Methanobacterium* grown over a range of pHs with $CaCO_3$ (green boxes) and HCO_3 (blue circles) as carbon sources. Isotope values for CH_4 from Oman wells NSHQ04 and NSHQ14 from January 2014, 2015 and 2016 are in black triangles. The fields for various methane isotope values are general approximations based on the diagram from Etiope (2016), (1–3) and do not represent the full range of diversity of these values, but serve as a general representation. The dashed line shows the common demarcation for abiogenic vs microbial methane. (For interpretation of the references to colour in this figure legend, the reader is referred to the web version of this article.)

following equations (Mook, 1986) (SI Text 1). The resulting isotopic composition of each part of the DIC pool based on pH and carbon species is shown in Supplementary SI Fig. 2. The fractionation factor calculations for $NaHCO_3$ vials are summarized in Table 1. The observed $\alpha_{HCO3/CH4}$ and resulting $\alpha_{CO2/CH4}$ for $NaHCO_3$ vials vary from 1.054 to 1.088 and 1.047 to 1.081, respectively.

The fractionation between δD_{H2O} and δD_{CH4} was also calculated and shows that the $\alpha_{H2O/CH4}$ varies from 1.458 to 1.656 for the $NaHCO_3$ vials. This was calculated by modifying Eq. (1), replacing $\delta^{13}C_{CH4}$ with δD_{CH4} and $\delta^{13}C_{CO2(aq)}$ with δD_{H2O}. δD_{H2O} was measured as −108‰ in NSHQ04 medium.

3.3. Hydrogen and carbon fractionation factor calculations for $CaCO_3$ vials

Fractionation factors for $CaCO_3$ vials ($\alpha_{CaCO3/CH4}$, $\alpha_{CO2/CH4}$, and $\alpha_{H2O/CH4}$) were calculated following a similar approach. The measured $\alpha_{CaCO3/CH4}$ and estimated $\alpha_{CO2/CH4}$ vary from 1.028 to 1.078 and 1.028 to 1.079, respectively, and $\alpha_{H2O\text{-}CH4}$ from 1.473 to 1.595 (Table 1). However, in order to calculate $\delta^{13}C_{CO2}$ values, we needed to calculate the amount of CO_2 in the vials as before. The $CaCO_{3(s)}$ is sparingly soluble at high pHs, and the amount of aqueous DIC pool varies orders of magnitude across the range of experimental pH (see SI Fig. 3). To first order, the CO_3^{2-} concentration is fixed by the K_{sp} and αCa^{2+} in the NSHQ04 medium. With 6 mM Ca^{2+} in the initial medium, the equilibrium dissolved CO_3^{2-} concentration is $\sim 10^{-6.25}$ (0.57 μM), and the resulting speciation of all aqueous carbon species can be calculated based on this fixed amount of CO_3^{2-} (SI Fig. 3). It is important to note that this is the initial equilibrium state of the medium, which will then be perturbed when methanogens are present and utilizing $H_2CO_{3(aq)}$. Consumption of $H_2CO_{3(aq)}$ during methanogenesis will induce further $CaCO_3$ dissolution, at a rate that is dependent upon pH and the degree of undersaturation. The fractionation factors for $\alpha_{CO2/CH4}$ reported in Table 1 are based on calculations with DIC in equilibrium with the $CaCO_3$ pool.

3.4. Gibbs free energy calculations

We calculated how much energy is available to the methanogens at the time the headspace gas was sampled for isotope measurements (2), which is based on the aqueous methanogenesis equation (3):

$$\Delta G = \Delta G^{\circ} + RT \ln Q \quad (2)$$

$$4H_{2(aq)} + H_2CO_{3(aq)} = CH_{4(aq)} + 3H_2O_{(l)} \quad (3)$$

ΔG^o is −193.01 kJ/mol at STP and pH 7 (Robie et al., 1978). The van't Hoff equation was used to calculate ΔG^o under experimental conditions when temperature (T) is 313.15 K (40 °C), which increases ΔG^o to −214.33 kJ/mol. R (ideal gas constant) is $8.314e^{-3}$ kJ/mol * K. Q is defined as:

$$Q = \{H_2O\}^3\{CH_4\}/\{H_2CO_3\}\{H_2\}^4 \quad (4)$$

where $\{H_2O\} = 1$, and all the species in the gas concentrations are calculated in their aqueous form, determined by using a dimensionless Henry's constant of 0.035 for CH_4 and 0.019 for H_2 (Sander, 2015), calculated at 25 °C. H_2CO_3 concentrations were calculated as previously described. The Gibbs free energy results for both $NaHCO_3$ and $CaCO_3$-amended experiments are shown in Table 2.

For the $NaHCO_3$-amended experiment, the Gibbs free energy calculation shows decreasing energy for CH_4 formation as pH increases. For the $CaCO_3$-amended experiment, there is a similar trend in decreasing Gibbs free energy as the pH increases. However, the energetics are less favorable overall than in the $NaHCO_3$-amended experiment since there are always orders of magnitude less H_2CO_3 available at any given pH (See SI Figs. 2 and 3).

3.5. Steady state model for $NaHCO_3$ carbon fractionation

We generated a steady state model to describe the carbon isotope fractionation during CH_4 production in the experiments buffered by $NaHCO_3$ (SI Fig. 4) that assumes there is a significant excess of carbon available for the microorganisms. The bioavailable aqueous carbon species that diffuses into the cell is H_2CO_3, with a $\delta^{13}C_{H2CO3}$ value that is established according to Supplemental equations (1)–(6) (SI equations). We assume that the process of diffusion in the aqueous phase does not impart a significant carbon isotope fractionation compared to methanogenesis (typically 0.7–0.8 permil, O'Leary, 1984). However, the rates of CO_2 uptake and escape from the cell can affect the observed net fractionation and need to be considered when evaluating the $\delta^{13}C$ of the intracellular CO_2. Thus, solving this model yields the equation:

$$\delta^{13}C_{CH4} = \delta^{13}C_{H2CO3} + (f_{esc} * \varepsilon_{red})/(1 + f_{esc}) \quad (5)$$

$$\varepsilon_{H2CO3-CH4} = -(f_{esc} * \varepsilon_{red})/(1 + f_{esc}) \quad (6)$$

with the parameter

$$f_{esc} = \frac{\phi_{esc}}{\phi_{red}} \quad (7)$$

f_{esc} relates the flux of CO_2 escape from the cell to the rate of CO_2 reduction to CH_4 in the cell. ε_{red} is the maximum observed enzymatic fractionation expected in the experiments, which we define as −78‰, based on the largest epsilon value observed for the $CaCO_3$ experiments. Although any particular mechanistic relationship between changes in f_{esc} and pH cannot be inferred from the available data, the observed isotopic fractionation (Table 1) evaluated in the context of this first order model suggests a link between increasing f_{esc} (from 1.4 to 24) and increasing culture pH as illustrated in SI Fig. 5. Increasing f_{esc} values signify that the rate of CH_4 production is slowing relative to the rate of CO_2 diffusing out of the cell, which suggests that intracellular CO_2 is converted less efficiently at higher pH.

3.6. Steady state model for $CaCO_3$-amended experiments

The $CaCO_3$-amended experiments explore a more complex system, where dissolved inorganic carbon

Table 2
Gibbs free energy calculations per mol CH_4 produced in $NaHCO_3$ and $CaCO_3$ experiments. Aqueous CH_4 and H_2 values reflect molar (M) concentrations when gas was extracted for isotopic analysis. H_2CO_3 values (M) were calculated based on pH of vials at time of sampling and total carbon added to vials (SI Figs. 2 and 3). Q was calculated with molar concentrations, not activities, because the values do not vary significantly for aqueous gases.

pH	$[CH_4](aq)$	$[H_2](aq)$	$[H_2CO_3](aq)$	Q	Gibbs free energy (kJ/mol CH_4)
$NaHCO_3$					
7.2	4.86E−11	4.90E−08	1.12E−03	7.55E+21	−83.2
7.4	6.71E−11	4.09E−08	7.35E−04	3.25E+22	−79.4
7.7	7.63E−11	1.85E−08	3.82E−04	1.72E+24	−69.0
8.2	5.09E−11	5.15E−08	1.23E−04	5.85E+22	−77.8
9.3	9.64E−11	1.87E−09	9.08E−06	8.59E+29	−34.9
9.6	2.00E−11	8.74E−10	4.18E−06	8.22E+30	−29.0
10.01	9.29E−11	1.24E−09	9.72E−07	4.09E+31	−24.8
$CaCO_3$					
7.06	6.02E−11	1.07E−08	1.42E−04	3.23E+25	−61.4
7.29	7.36E−11	4.79E−09	8.94E−05	1.56E+27	−51.3
7.77	6.59E−11	6.79E−08	3.56E−06	8.74E+23	−70.8
8.97	4.90E−12	1.91E−07	2.25E−08	1.63E+23	−75.2
8.87	7.17E−11	2.02E−08	3.56E−08	1.22E+28	−46.0
9.23	8.98E−11	2.88E−09	8.94E−09	1.45E+32	−21.5

concentrations at any given pH are controlled by the rate and extent of $CaCO_3$ dissolution. The fluxes of carbon affected by carbonate dissolution and precipitation are therefore incorporated as additional components to the steady-state model (Fig. 4). Carbonate dissolution affects the rates of diffusion of CO_2 into and out of the cell, which must be compared to rates of CO_2 reduction to CH_4. Initially, the extent of calcium carbonate dissolution necessary to establish equilibrium for the DIC pool is dependent upon pH (see SI Fig. 3). Before the methanogens start consuming CO_2, the forward flux of carbonate dissolution is balanced by carbonate precipitation. Once methanogenesis proceeds, the excess $CaCO_{3(s)}$ can dissolve to restore equilibrium when CO_2 is consumed by cellular uptake and methane production. The CO_2 portion of the DIC pool is isotopically offset from the total pool, as described in Eq. (5). This CO_2 diffuses into and out of the cell (assumed without significant net fractionation). Some fraction of this CO_2 is enzymatically reduced to produce intracellular CH_4 with a kinetic carbon isotope effect. The generated CH_4 subsequently accumulates in the extracellular medium and headspace from where it is measured. Solving the steady-state model (SI Fig. 4) yields the following net isotope fractionation between the mineral substrate and resulting methane:

$$\varepsilon_{CaCO3/CH4} = \frac{(\varepsilon_{CO3^{2-}/DIC} - \varepsilon_{CO2/DIC})}{(f_{precip}+1)} - \frac{f_{precip} f_{esc} \varepsilon_{red}}{(f_{esc}+1)(f_{precip}+1)} \quad (8)$$

with the parameters defined by Eq. (7) and:

$$f_{precip} = \frac{\phi_{precip}}{\phi_{red}} \quad (9)$$

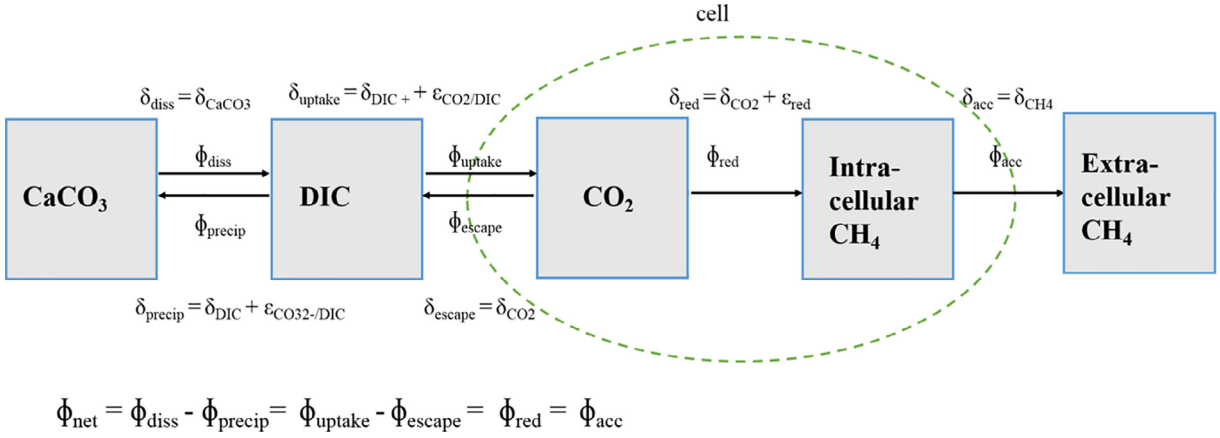

Fig. 4. Steady state model illustrating the various carbon fluxes and their isotopic compositions in the $CaCO_3$ experiments. From left to right: calcium carbonate dissolves (ϕ_{diss}) and carbon accumulates in the dissolved inorganic carbon (DIC) pool from where the carbonate (CO_3^{2-}) species can re-precipitate (ϕ_{precip}) and the CO_2 species can diffuse into the cell (ϕ_{uptake}) and back out (ϕ_{escape}) unless it is converted into CH_4 (ϕ_{red}) and subsequently accumulates in the extracellular medium and headspace. The measured isotopic composition is that of the accumulated extracellular CH_4, which was sampled from the headspace. The small isotopic effects associated with CH_4 diffusion through water and partitioning between dissolved and gaseous CH_4 do not have a significant effect and are excluded for clarity.

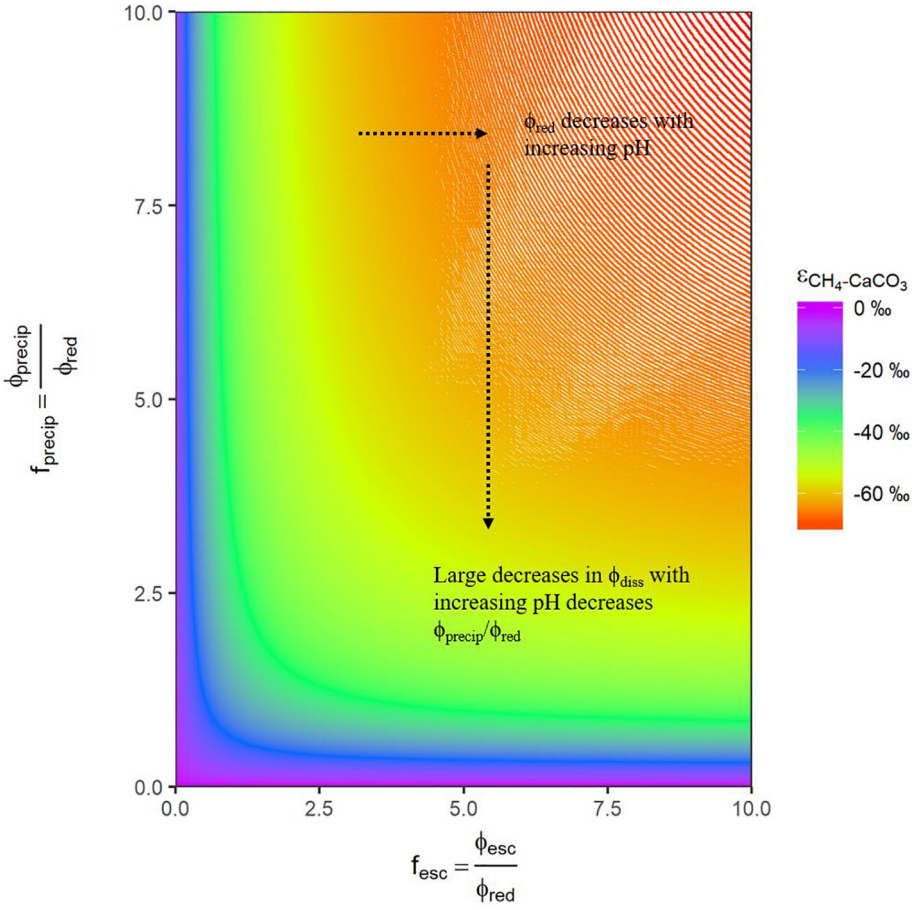

Fig. 5. Range of $\varepsilon(CH_4 - CaCO_3)$ values obtained from varying the rate of CO_2 escape from the cell (ϕ_{escape}) and the rate of carbonate re-precipitation (ϕ_{precip}) both relative to the methane production rate (ϕ_{red}).

$\varepsilon_{CO2\text{-}DIC}$ is the fractionation between the original $CaCO_3$ carbon source and the bioavailable form of carbonate, H_2CO_3, which diffuses into the cell. $\varepsilon_{CO3\text{-}DIC}$ is the fractionation of the CO_3^{2-} portion of the carbon pool when it back-precipitates as a carbonate mineral at high pHs. ε_{red} is the intrinsic fractionation of the enzymatic CO_2 reduction, which we estimate at −78‰ using the maximum observed fractionation in the $NaHCO_3$ experiments.

Fig. 5 illustrates the range of overall fractionation factors predicted by this model for f_{esc} and f_{precip} values between 0 (no CO_2 escape from the cell/no carbonate re-precipitation) and 10 (CO_2 flux escaping the cell exceeds CO_2 reduction by 10:1/carbonate re-precipitation flux exceeds CO_2 reduction by 10:1). Suppressed net fractionations are predicted for small f_{esc} and f_{precip} values. The predicted ε is <30‰ when the flux of carbon that undergoes irreversible reduction to methane (ϕ_{red}) comprises the majority of the total C that is released from carbonate dissolution, thus leading to small f_{precip} values. This also occurs when most of the carbon is reduced to methane versus diffusing out of the cell (ϕ_{esc}), leading to small f_{esc} values (Fig. 5). In contrast, when f_{precip} or f_{red} are above ~5, there are large fractionations when the rate of reduction is slow compared to rates of precipitation and escape.

4. DISCUSSION

4.1. Large variations in C isotope fractionation by Methanobacterium NSHQ4. depending upon C source and pH

We simulated abundant carbon availability in the $NaHCO_3$-amended experiments and variable carbon limitation in the $CaCO_3$-amended experiments to characterize the diverse environments in which methanogens grow under alkaline conditions. In the $NaHCO_3$-amended experiments, the maximum carbon isotope fractionation increased as the rate of methane production decreased at high pH (Fig. 2). Physiological adaptations are expected to occur as pH increases, since it is more challenging to maintain a proton motive force, which causes organisms to expend more energy to produce ATP, in turn leading to slower growth rates. Typically, slower growth rates are associated with larger expressed isotope fractionation (Zyakun, 1996). The ΔG of methane formation for $NaHCO_3$-amended experiments also decreased as a function of pH, primarily due to low $CO_{2(aq)}$ (Table 2). In general, as the ΔG decreases under environmental conditions, there is increased C kinetic isotope effect in the reduction of CO_2 to CH_4 (Valentine et al., 2004; Penning et al., 2005; Takai et al., 2008). However, this effect is usually observed as pH

decreases instead of pCO_2. For example, maximum $\delta^{13}C_{CH4}$ depletion is only observed in methane when hydrogenophilic methanogens are being sustained close to the minimum free energy yield e.g. (Hoehler et al., 2000), and the $\alpha_{CO2/CH4}$ is significantly reduced at high partial pressures of H_2. Therefore, it has been suggested that the $\delta^{13}C_{CH4}$ could be used as a diagnostic indicator of the energy state of microbial communities *in-situ* (Hoehler et al., 2000). However, the $CaCO_3$-amended experiments display notably suppressed carbon fractionation around pH 9, which is not predicted by the decreasing ΔG values.

The steady state model of the $NaHCO_3$-amended experiments illustrates that the resulting $\delta^{13}C_{CH4}$ is dependent on the value of ε_{red} associated with methanogenesis, the starting isotopic composition of the bioavailable carbon, and the rates of CO_2 escape and uptake into the cell (SI Fig. 4). It is important to note that this model assumes that the culture growth can be approximated to be in a quasi steady state, and that the methanogenesis reaction is practically irreversible under the experimental conditions we tested. It also assumes that the produced CH_4 equilibrates with the extracellular pool of CH_4, and that the different inorganic carbon species in the DIC pool equilibrate isotopically on time scales faster than the concomitant rates of methane generation. This model can explain the observed $\delta^{13}C_{CH4}$ values that range from −50 to −80‰ similar to the experimental pH range (Fig. S5).

In predicting carbon isotope fractionations during methanogenesis, the possibility of enzymatic reversibility must be considered for each step associated with methanogenesis, including the final step catalyzed by methyl-coenzyme M reductase (MCR) (Valentine et al., 2004; Thauer, 2011; Scheller et al., 2013). Valentine et al. (2004) proposed that the Gibbs free energy controls the magnitude of reversibility, which is primarily controlled by H_2 partial pressure. Experiments by Valentine et al. (2004) show that abundant H_2 leads to larger Gibbs free energy values, less carbon fractionation, and limited reversibility. In contrast, limited H_2 leads to smaller Gibbs free energy values approaching zero, larger expressed carbon fractionation, and presumably more reversibility. This suppresses kinetic equilibrium effects, and instead leads to maximum expressed carbon fractionation, which Zyakun (1996) predicts to be 100‰ for methanogenesis.

The $CaCO_3$-amended experiments were also modeled assuming steady state conditions (Fig. 4). However, we cannot calculate exact f_{precip} and f_{red} values for these experiments because the system is under constrained without specific rate measurements (e.g. we did not quantify the cell specific rate of CO_2 reduction, which is important for quantifying key fluxes at each node). To be fully predictive, we would also need to be able to quantify the absolute carbonate dissolution and re-precipitation fluxes. Instead, we use the model to explore the boundary conditions for C isotope variation and potential f_{precip} and f_{red} values consistent with our experimental observations. Small overall fractionation factors $\varepsilon_{CaCO3/CH4}$ are predicted when either f_{precip} or f_{red} are minimized (Eq. (8)). The largest fractionation occurs around pH 7–8 when there are high methane production rates and ϕ_{red} is large. However, in these experiments, the CH_4 production rate at pH 9 drops by an order of magnitude from its maximum rate. Changes in ϕ_{red} cannot explain the suppressed fractionation at high pH. Instead, we infer that the system has reached a critical threshold in terms of the flux of bioavailable carbon provided by carbonate dissolution, leading to limited concentrations of bioavailable carbon as the solubility and rates of $CaCO_3$ decrease with increasing pH (Chou et al., 1989; Pokrovsky and Schott, 1999). Thus, due to a limited carbon pool, *Methanobacterium NSHQ4* is consuming nearly all of the available CO_2, which suppresses isotopic fractionation.

We compared the fractionation factors for *Methanobacterium NSHQ4* growing at alkaline pH to other known laboratory culture studies of methanogens producing CH_4 (Table 3). The maximum CO_2-CH_4 fractionation factors vary from 1.025 to 1.095 across a variety of studies (Games et al., 1978; Balabane et al., 1987; Whiticar, 1999; Chasar et al., 2000; Chidthaisong et al., 2002; Kohl et al.,

Table 3
Fractionation factors for various species of *Methanobacterium*.

Organism	Substrate	Temperature (°C)	Reference	Max $^{13}\alpha_{CO2\text{-}CH4}$	Max $^{2}\alpha_{H2O\text{-}CH4}$
Methanogen fractionation factors					
Methanobacterium NSHQ4	**H_2/CO_2**	**40**	**This paper**	**1.076**	**1.354**
Methanobacterium thermoautotrophicum	H_2/CO_2	65	Games et al. (1978)	1.025	NA
Methanobacterium bryantii	H_2/CO_2	40	Games et al. (1978)	1.061	NA
Methanobacterium formicicum	H_2/CO_2	34	Balabane et al. (1987)	1.055	1.674
Methanobacterium strain MoH	H_2/CO_2	40	Games et al. (1978)	1.061	NA
Methanobacterium spp. from rice soil	H_2/CO_2	30	Chidthaisong et al. (2002)	1.052	1.65
Methanobacterium spp. from rice roots	H_2/CO_2	30	Chidthaisong et al. (2002)	1.06	1.86
Methanogens (unspecified culture)	H_2/CO_2	NA	Whiticar (1999)	1.055–1.058	NA
Unspecificed Methanogen culture	H_2/CO_2	NA	Whiticar (1999)	1.049–1.095	1.16
Unspecificed Methanogen	H_2/CO_2	NA	Chasar et al (2000)	1.06–1.08	1.25–1.35
High pH methanogens					
Unidentified methanogen (growing at high pH)	H_2/CO_2		Kohl et al. (2016)	1.078	1.5

2016). In this study, the maximum $\alpha_{CO2\text{-}CH4}$ is 1.076. When considering $\alpha_{H2O\text{-}CH4,}$ we note that it is the δD of the water, not the initial H_2, that controls the δD of CH_4 produced from CO_2-reduction (e.g. Daniels, 1980; Valentine et al., 2004). There is less data available for $\alpha_{H2O\text{-}CH4}$ for diverse methanogens, and the range is much broader from 1.16 to 1.86; our calculated $\alpha_{H2O\text{-}CH4}$ is 1.354, in the middle of the range. Thus, *Methanobacterium NSHQ4* growing at high pH in culture does not have significantly different hydrogen isotopic fractionation factors than other methanogens.

4.2. Environmental relevance

Our results demonstrate that both highly depleted and relatively enriched $\delta^{13}C_{CH4}$ is produced by *Methanobacterium NSHQ4* under carbon limitation at high pH. The carbon isotope fractionation depends on the degree of carbon limitation. In the $NaHCO_3$ experiments, although $CO_{2\,(aq)}$ is low at pH 9 and above, there is orders of magnitude more DIC than in the experiments that are buffered by $CaCO_3$ dissolution. Slow methane generation, in conjunction with abundant DIC, leads to increased carbon fractionation at high pH.

When interpreting CH_4 isotopes from hyperalkaline environments, it is important to consider the carbon source and availability. For example, soda lakes are in contact with atmospheric CO_2 (Oremland et al., 1987), and shallow subsurface systems are often open with respect to CO_2 (Morrill et al., 2013). However, many systems are often not appreciably supplied with atmospheric CO_2. From this work, it is reasonable to predict very large (>50‰) increases in $\delta^{13}C_{CH4}$ in rock-hosted systems where DIC is low but the rocks are partly carbonated and can continually provide a small, slow source of CO_2 to sustain methanogenesis when H_2 is available. Thus, when we evaluate high pH fluids from closed systems with long residence times, we must consider whether methanogens may be utilizing carbonate-derived carbon. For example, even though subsurface alkaline fluids in Oman contain little DIC, there are widespread carbonate veins in the peridotite (Kelemen et al., 2011). The $\delta^{13}C_{CH4}$ produced under these conditions would strongly overlap with the traditionally interpreted "abiogenic" methane field (e.g. in Fig. 3). Microbiology may be significantly contributing to CH_4 production in ways that cannot be easily discerned from isotope systematics.

4.3. Significance of carbon and hydrogen isotope values of CH_4 in hyperalkaline fluids

It is challenging to determine the source of dissolved methane detected in hyperalkaline fluids. The Samail Ophiolite in Oman, including the CH_4 detected in well NSHQ04 from which the *Methanobacterium NSHQ4* were isolated (Miller et al. 2016), contains positive $\delta^{13}C_{CH4}$ values (+2.4 and +3‰). As discussed by Etiope (2016) and Miller et al. (2017), the methane from these serpentinites is typically classified as abiogenic. The methane is inferred to have formed through low-temperature, metal catalyzed FTT-type or Sabatier reactions, even though such reactions have not been directly observed under the hydrated and low-temperature conditions that persist in serpentinite aquifers.

However, the results of this study suggest that the relatively positive $\delta^{13}C_{CH4}$ values observed in the Samail ophiolite are higher than feasible through methanogenesis alone. Subsurface carbonate veins from Oman have $\delta^{13}C_{VPDB}$ values ranging from −1.48 to −7.05‰ (Clark and Fontes, 1990; Kelemen and Matter, 2008; Kelemen et al., 2011; Mervine et al., 2014; Miller et al., 2016), and so even in the extreme case that all dissolving carbonate were immediately converted to CH_4, the $\delta^{13}C_{CH4}$ values could reach the same values as the rock-hosted carbon pool, but not more positive. Thus another mechanism in addition to, or besides, methanogenesis, must be invoked.

It is worthwhile to explore the effect of potential aerobic and/or anaerobic methane oxidation on the isotopic composition of the residual methane, if we start our calculations with the most elevated microbial $\delta^{13}C_{CH4}$ observed at high pH in our $CaCO_3$ experiments. Progressive oxidation of this microbially produced CH_4 was modeled assuming a closed, irreversible system with Rayleigh distillation. No additional methanogenesis was permitted to occur. The initial $\delta^{13}C$ and δD values of the CH_4 used in the calculations were −27.6‰ and −410‰, respectively, based on values from *Methanobacterium NSHQ4* $CaCO_3$ cultures at ~pH 9. It is important to note that the δD_{H2O} of fluid from Oman varies from −15 to +3‰ (average −6‰), whereas the laboratory water δD_{H2O} is −108‰, which makes it hard to directly compare our calculations to the environmental data. To account for this difference, we used the average $\alpha_{H2O/CH4}$ of 1.523 to calculate a starting δD_{CH4} is −347‰. This simply assumes the hydrogen in the methane is in equilibrium with Oman water vs. experimental water. We then assume this CH_4 is subsequently oxidized by an unknown methane oxidizer, by applying two different potential fractionation factors for aerobic and anaerobic methane oxidation. The model is closed and unidirectional with the consumption of CH_4 to CO_2 without additional or concurrent CH_4 production.

The equations used were standard Rayleigh distillation equations applied to methane oxidation, as briefly summarized below:

$$\delta^{13}C_{CH_4} = \delta^{13}C_{CH_4^\circ} + \varepsilon * \ln[CH_4]/[CH_4]_{total} \quad (10)$$

$$\delta^{13}C_{CO_2} = \delta^{13}C_{CH_4^\circ} - \varepsilon * \frac{[CH_4]/[CH_4]_{total}}{1 - [CH_4]/[CH_4]_{total}} * ln[CH_4]/[CH_4]_{total} \quad (11)$$

where $\varepsilon = (\alpha - 1) * 1000$, the ratio of CH_4 shows how much CH_4 has been consumed relative to the total starting amount, and δCH_{4o} is the initial value of CH_4 in the system. The fractionation factors used in the model ranged from $\alpha_{CH4/CO2} = 1.012$ to 1.039 and $\alpha_{CH4/H2O} = 1.109$ to 1.315 (Holler et al., 2009). These values encompass data for both anaerobic and aerobic carbon fractionation. Methanotrophs such as *Methylococcus* sp. that utilize methane monooxygenase have been detected in the subsur-

face CH_4 rich fluids in Oman (Miller et al., 2016). It is not apparent if anaerobic methane oxidation processes are occurring in the subsurface fluids. Methane oxidation utilizing nitrate, sulfate and Fe(III)-oxides is thermodynamically favorable *in-situ*, but known anaerobic methane oxidizing organisms such as ANME have not been detected in 16S rRNA sequencing of biomass (Miller et al. 2016; Rempfert et al. 2017). The anaerobic carbon fractionation values were obtained from measuring CH_4 consumed by enrichment cultures of anaerobic sea sediments (Holler et al., 2009). These are some of the few experimental values provided for anaerobic methane oxidation, and they align with fractionation factor estimates proposed by other authors (Valentine et al., 2004; Conrad, 2005).

Although methanogenesis alone cannot generate relatively high $\delta^{13}C_{CH4}$ and δD_{CH4} observed in subsurface fluids in Oman, subsequent methane oxidation of microbially produced methane could lead to these values (Fig. 6). The most conservative $\alpha_{CH4/CO2}$ 1.012 for $\delta^{13}C_{CH4}$ would produce the maximum measured $\delta^{13}C_{CH4}$ of 3‰ when >75% of the original CH_4 was consumed. However, if the 1.039 carbon isotope fractionation factor is applied, the residual $\delta^{13}C_{CH4}$ value of +3‰ is achieved by consuming only slightly over 50% of the original CH_4. The δD_{CH4} models are similar. The initial δD_{CH4} of −347‰ is increased during oxidation along a steeper slope than $\delta^{13}C_{CH4}$. In order to obtain δD_{CH4} values measured in subsurface wells from Oman (−200‰) ~75% of the CH_4 would be consumed in the upper limit case, where $\alpha_{CH4/H2O}$ is 1.315. In the conservative case ($\alpha_{CH4/H2O}$ is 1.109). Approximately 30% of the CH_4 would be consumed to produce the observed δD_{CH4}.

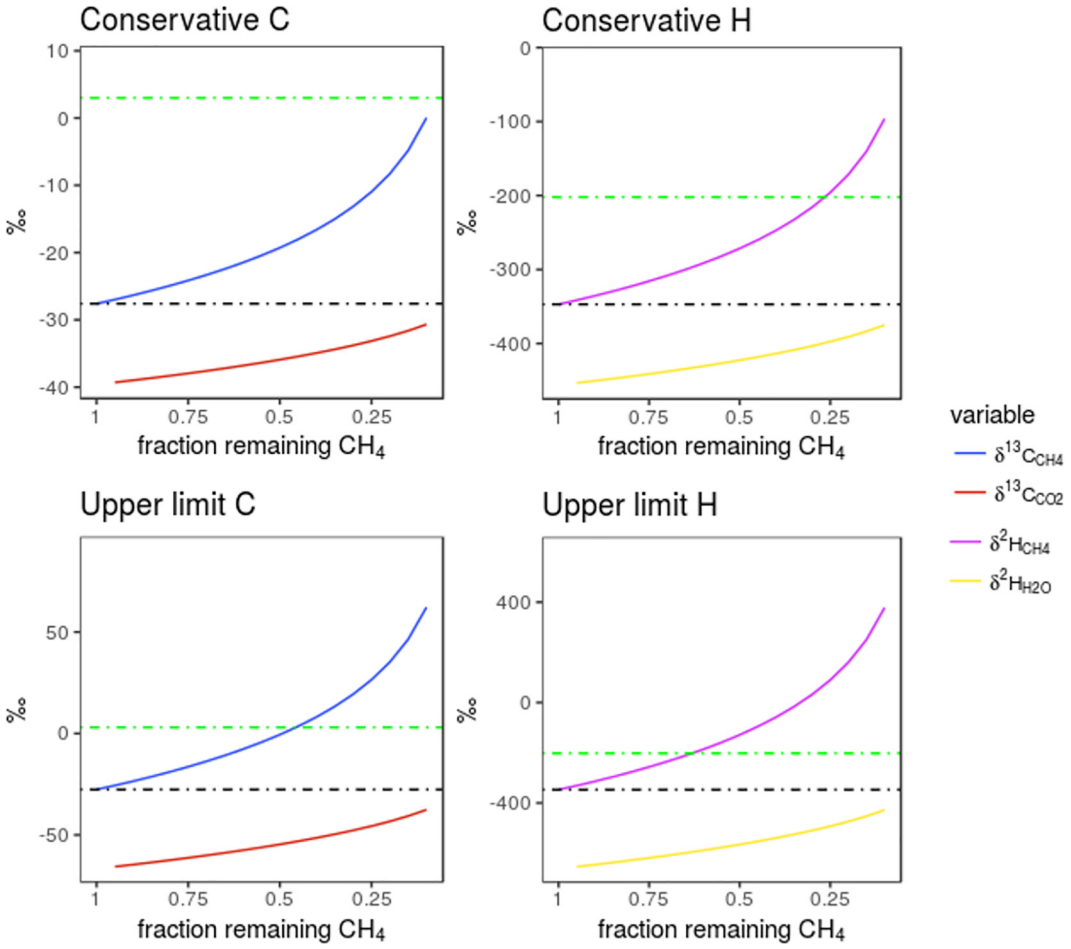

Fig. 6. Expected changes in $\delta^{13}C$ and δD of residual CH_4 during incremental closed-system oxidation under two different fractionation factors scenarios. Initial value of $\delta^{13}C$ is −27.6‰ and δD is −347‰, as indicated by the solid black lines. Conservative C fractionation factor $\alpha_{CH4/CO2}$ is 1.012 (=12‰) and upper limit $\alpha_{CH4/CO2}$ is 1.039 (=39‰). Conservative H fractionation factor $\alpha_{CH4/H2O}$ is 1.109 (109‰) and upper limit H $\alpha_{CH4/H2O}$ is 1.315 (315‰). Fractionation factors are taken from Holler et al. (4). Dashed green lines indicate the $\delta^{13}C$ and δD values of methane (+3‰ and −200‰, respectively) that have been measured from subsurface fluids rich in CH4 in an Oman hyperalkaline serpentinite aquifer. The isotopic composition shown for the accumulated product (CO_2 and H_2O, respectively in blue) represents only the pool released from methane oxidation and not any mixing with pre-existing sources of CO_2 and H_2O. (For interpretation of the references to colour in this figure legend, the reader is referred to the web version of this article.)

5. CONCLUSIONS

We report CO_2-CH_4 and H_2O-CH_4 fractionation factors for *Methanobacterium NSHQ4* growing at alkaline pH with both sodium bicarbonate and calcium carbonate as a carbon source. The hydrogen fractionation factors in both experiments are similar, with an average $\alpha_{H2O\text{-}CH4}$ of 1.309. However, the range of expressed carbon isotope fractions is much larger ($\alpha_{CO2\text{-}CH4}$ 1.045–1.075). The expressed carbon fractionation factors of organisms consuming $NaHCO_3$ increases with increasing pH, resulting in increasingly negative $\delta^{13}C_{CH4}$ as low as −85‰. Up to pH ~ 8.9, $CaCO_3$ experiments also display a trend of increased carbon isotope fractionation with increasing pH. However, near pH 9 in carbonate-fed experiments, carbon isotope fractionation is suppressed, resulting in $\delta^{13}C_{CH4}$ values as high as −28‰. This is a more positive $^{13}C_{CH4}$ than typically observed in methanogenesis (Whiticar, 1999). However, it only occurs when $CaCO_3$ is a carbon source for methanogenesis at high pH when carbon availability is controlled by carbonate dissolution dynamics.

To expand upon our laboratory data, we modeled expected $\delta^{13}C_{CH4}$ values in high pH environments by using observed fractionation factors and variable rates of CO_2 uptake and reduction. If bioavailable carbon is not limited and *Methanobacterium NSHQ4* is growing slowly in fluids >pH 9, the resulting CH_4 produced by methanogenesis would show large carbon isotope fractionation. It would be ~70‰ more depleted in $^{13}C_{CH4}$ than the source carbon. If dissolved H_2, CO_2 and CH_4 are close to thermodynamic equilibrium, the resulting $^{13}C_{CH4}$ could be depleted up to −100‰ relative to the initial carbon source (Zyakun 1996). If carbon is derived from carbonate mineral dissolution at pH > 9, and dissolution limits methane generation, then the resulting carbon fractionation is suppressed. This is due to microbes consuming most of the bioavailable carbon and is limited by the rate of carbon dissolution at high pH.

Methanogenesis at high pH and under carbon-limited conditions, when paired with a later, separate stage of methane oxidation, can lead to unusually positive $\delta^{13}C_{CH4}$ and δD_{CH4} values. We calculated the effects of oxidation of methane, starting with the heavier carbon and isotope values observed in high pH and carbon-limited conditions in the laboratory. Modeling shows it is possible to oxidize ~50% of CH_4 with a $\delta^{13}C_{CH4}$ values of −28‰ to produce a residual $\delta^{13}C_{CH4}$ of +2‰, as measured from subsurface wells in Oman.

Importantly, methanogenesis can proceed under highly C limited conditions utilizing $CaCO_3$ as a carbon source, even at high pH. Methane isotope compositions contain valuable information regarding environmental conditions of methane formation, but as this study shows, they cannot be used alone to preclude microbial activity. We suggest that microbial processes may quantitatively contribute to methane production in rock-hosted aquifers, including within systems that have previously been inferred to be dominated by "abiogenic" methane for which there is no proven mechanism of formation. With growing evidence of modern-day CH_4 releases of methane on Mars (Mumma et al., 2009; Webster et al., 2015), as well as CH_4 detected in hyperalkaline plumes on Enceladus (Waite et al., 2006; Waite et al., 2017), it is vital to understand that it should at least be possible to support microbial methane formation in hyperalkaline serpentinizing systems on Earth, if sufficient dissolved inorganic carbon or mineral carbonates are present to serve as a carbon source.

ACKNOWLEDGEMENTS

We would like to thank Peter Kelemen and Juerg Matter for their ongoing collaborations in the analysis and interpretation of fluid chemistry and microbiology in the Samail Ophiolite. Boswell Wing and Daniel Nothaft provided constructive feedback about the experimental work. We would like to thank the Fierer lab at the University of Colorado at Boulder for assistance in sequencing the 16S rRNA amplicons for the microbial consortia. This research was funded by the Department of Energy (DE-SC0006886) and the NASA Astrobiology Institute (Cooperative Agreement NNA15BB02A). Work at Lawrence Berkeley National Laboratory was supported by a grant from the US Department of Energy, Office of Science, Office of Basic Energy Sciences, Chemical Sciences, Geosciences Division under Award Number DE-AC02-05CH11231.

REFERENCES

Abrajano T. A., Sturchio N. C., Kennedy B. M., Lyon G. L., Muehlenbachs K. and Bohlke J. K. (1990) Geochemistry of reduced gas related to serpentinization of the Zambales ophiolite, Philippines. *Appl. Geochem.* **5**, 625–630.

Balabane M., Galimov E., Hermann M. and Létolle R. (1987) Hydrogen and carbon isotope fractionation during experimental production of bacterial methane. *Org. Geochem.* **11**, 115–119.

Barnes I., LaMarche V. C. and Himmelberg G. (1967) Geochemical evidence of present-day serpentinization. *Science* **156**, 830–832.

Barnes I., O'Neil J. R. and Trescases J. J. (1978) Present day serpentinization in New Caledonia, Oman and Yugoslavia. *Geochim. Cosmochim. Acta* **42**, 144–145.

Benjamin M. M. (2002) *Water Chemistry*. Waveland Press Inc., Long Grove, Illinois.

Blank J. G., Green S. J., Blake D., Valley J. W., Kita N. T., Treiman A. and Dobson P. F. (2009) An alkaline spring system within the Del Puerto Ophiolite (California, USA): a Mars analog site. *Planet. Space Sci.* **57**, 533–540.

Bradley A. S. and Summons R. E. (2010) Multiple origins of methane at the Lost City Hydrothermal Field. *Earth Planet. Sci. Lett.* **297**, 34–41.

Brass M. and Röckmann T. (2010) Continuous-flow isotope ratio mass spectrometry method for carbon and hydrogen isotope measurements on atmospheric methane. *Atmospheric Meas. Tech.* **3**, 1707–1721.

Chapelle F. H., O'Neill K., Bradley P. M., Methé B. A., Ciufo S. A., Knobel L. L. and Lovley D. R. (2002) A hydrogen-based subsurface microbial community dominated by methanogens. *Nature* **415**, 312–315.

Chasar L. S., Chanton J. P., Glaser P. H. and Siegel D. I. (2000) Methane concentration and stable isotope distribution as evidence of rhizospheric processes: comparison of a fen and bog in the glacial lake agassiz Peatland complex. *Ann. Bot.* **86**, 655–663.

Chidthaisong A., Chin K.-J., Valentine D. L. and Tyler S. C. (2002) A comparison of isotope fractionation of carbon and hydrogen from paddy field rice roots and soil bacterial

enrichments during CO_2/H_2 methanogenesis. *Geochim. Cosmochim. Acta* **66**, 983–995.
Chou L., Garrels R. M. and Wollast R. (1989) Comparative study of the kinetics and mechanisms of dissolution of carbonate minerals. *Chem. Geol.* **78**, 269–282.
Clark I. D. and Fontes J.-C. (1990) Paleoclimatic reconstruction in northern Oman based on carbonates from hyperalkaline groundwaters. *Quat. Res.* **33**, 320–336.
Conrad R. (2005) Quantification of methanogenic pathways using stable carbon isotopic signatures: a review and a proposal. *Org. Geochem.* **36**, 739–752.
Daniels L., Fulton G., Spencer R. W. and Orme-Johnson W. H. (1980) Origin of hydrogen in methane produced by Methanobacterium thermoautotrophicum. *J. Bacteriol.* **141**, 694–698.
Eecke H. C. V., Butterfield D. A., Huber J. A., Lilley M. D., Olson E. J., Roe K. K., Evans L. J., Merkel A. Y., Cantin H. V. and Holden J. F. (2012) Hydrogen-limited growth of hyperthermophilic methanogens at deep-sea hydrothermal vents. *Proc. Natl. Acad. Sci.* **109**, 13674–13679.
Ehlmann B. L., Mustard J. F. and Murchie S. L. (2010) Geologic setting of serpentine deposits on Mars: SERPENTINE ON MARS. *Geophys. Res. Lett.* **37**, n/a–n/a.
Etiope G. (2009) Natural emissions of methane from geological seepage in Europe. *Atmos. Environ.* **43**, 1430–1443.
Etiope G. (2016) Methane origin in the Samail ophiolite: Comment on "Modern water/rock reactions in Oman hyperalkaline peridotite aquifers and implications for microbial habitability". *Geochim. Cosmochim. Acta*, 217–241.
Etiope G., Ehlmann B. L. and Schoell M. (2013) Low temperature production and exhalation of methane from serpentinized rocks on Earth: a potential analog for methane production on Mars. *Icarus* **224**, 276–285.
Etiope G., Schoell M. and Hosgörmez H. (2011) Abiotic methane flux from the Chimaera seep and Tekirova ophiolites (Turkey): Understanding gas exhalation from low temperature serpentinization and implications for Mars. *Earth Planet. Sci. Lett.* **310**, 96–104.
Etiope G. and Sherwood Lollar B. (2013) Abiotic methane on earth. *Rev. Geophys.* **51**, 276–299.
Games L. M., HayesRobert J. M. and Gunsalus P. (1978) Methane-producing bacteria: natural fractionations of the stable carbon isotopes. *Geochim. Cosmochim. Acta* **42**, 1295–1297.
Glein C. R., Baross J. A. and Waite, Jr., J. H. (2015) The pH of Enceladus' ocean. *Geochim. Cosmochim. Acta* **162**, 202–219.
Hoehler T. M., Borowski W. S., Alperin M. J., Rodriguez N. M. and Paull C. K. (2000) Model, stable isotope, and radiotracer characterization of anaerobic methane oxidation in gas hydrate-bearing sediments of the Blake Ridge. In Proceedings of the Ocean Drilling Program, Scientific Results Ocean Drilling Program College Station, TX. pp. 79–85. Available at: http://www-odp.tamu.edu/publications/164_sr/volume/chapters/SR164_08.PDF [accessed October 9, 2015].
Holler T., Wegener G., Knittel K., Boetius A., Brunner B., Kuypers M. M. M. and Widdel F. (2009) Substantial 13C/12C and D/H fractionation during anaerobic oxidation of methane by marine consortia enriched in vitro. *Environ. Microbiol. Rep.* **1**, 370–376.
Kelemen P. B. and Matter J. (2008) In situ carbonation of peridotite for CO_2 storage. *Proc. Natl. Acad. Sci.* **105**, 17295–17300.
Kelemen P. B., Matter J., Streit E. E., Rudge J. F., Curry W. B. and Blusztajn J. (2011) Rates and mechanisms of mineral carbonation in peridotite: natural processes and recipes for enhanced, in situ CO_2 capture and storage. *Annu. Rev. Earth Planet. Sci.* **39**, 545–576.
Kiene R. P., Oremland R. S., Catena A., Miller L. G. and Capone D. G. (1986) Metabolism of reduced methylated sulfur compounds in anaerobic sediments and by a pure culture of an estuarine methanogen. *Appl. Environ. Microbiol.* **52**, 1037–1045.
Klein F., Humphris S. E., Guo W., Schubotz F., Schwarzenbach E. M. and Orsi W. D. (2015) Fluid mixing and the deep biosphere of a fossil Lost City-type hydrothermal system at the Iberia Margin. *Proc Natl. Acad. Sci.*, 201504674.
Kohl L., Cumming E., Cox A., Rietze A., Morrissey L., Lang S. Q., Richter A., Suzuki S., Nealson K. H. and Morrill P. L. (2016) Exploring the metabolic potential of microbial communities in ultra-basic, reducing springs at The Cedars, CA, USA: experimental evidence of microbial methanogenesis and heterotrophic acetogenesis. *J. Geophys. Res. Biogeosci.* **121**, 2015JG003233.
Komatsu G., Ori G. G., Cardinale M., Dohm J. M., Baker V. R., Vaz D. A., Ishimaru R., Namiki N. and Matsui T. (2011) Roles of methane and carbon dioxide in geological processes on Mars. *Planet. Space Sci.* **59**, 169–181.
Kotelnikova S., Macario A. J. and Pedersen K. (1998) Methanobacterium subterraneum sp. nov., a new alkaliphilic, eurythermic and halotolerant methanogen isolated from deep granitic groundwater. *Int. J. Syst. Bacteriol.* **48**, 357–367.
Kral T. A., Birch W., Lavender L. E. and Virden B. T. (2014) Potential use of highly insoluble carbonates as carbon sources by methanogens in the subsurface of Mars. *Planet. Space Sci.* **101**, 181–185.
Lollar B. S., Frape S. K., Weise S. M., Fritz P., Macko S. A. and Welhan J. A. (1993) Abiogenic methanogenesis in crystalline rocks. *Geochim. Cosmochim. Acta* **57**, 5087–5097.
Madigan M. T. (2012) *Brock Biology of Microorganisms*. Benjamin Cummings, San Francisco.
Mathrani I. M., Boone D. R., Mah R. A., Fox G. E. and Lau P. P. (1988) Methanohalophilus zhilinae sp. nov., an alkaliphilic, halophilic, methylotrophic methanogen. *Int. J. Syst. Bacteriol.* **38**, 139–142.
Mervine E. M., Humphris S. E., Sims K. W. W., Kelemen P. B. and Jenkins W. J. (2014) Carbonation rates of peridotite in the Samail Ophiolite, Sultanate of Oman, constrained through 14C dating and stable isotopes. *Geochim. Cosmochim. Acta* **126**, 371–397.
Miller H. M., Matter J. M., Kelemen P., Ellison E. T., Conrad M. E., Fierer N., Ruchala T., Tominaga M. and Templeton A. S. (2016) Modern water/rock reactions in Oman hyperalkaline peridotite aquifers and implications for microbial habitability. *Geochim. Cosmochim. Acta* **179**, 217–241.
Mook W. G. (1986) 13C in atmospheric CO_2. *Neth. J. Sea Res.* **20**, 211–223.
Morrill P. L., Kuenen J. G., Johnson O. J., Suzuki S., Rietze A., Sessions A. L., Fogel M. L. and Nealson K. H. (2013) Geochemistry and geobiology of a present-day serpentinization site in California: The Cedars. *Geochim. Cosmochim. Acta* **109**, 222–240.
Moser D. P., Gihring T. M., Brockman F. J., Fredrickson J. K., Balkwill D. L., Dollhopf M. E., Lollar B. S., Pratt L. M., Boice E., Southam G., Wanger G., Baker B. J., Pfiffner S. M., Lin L.-H. and Onstott T. C. (2005) Desulfotomaculum and Methanobacterium spp. Dominate a 4- to 5-kilometer-deep fault. *Appl. Environ. Microbiol.* **71**, 8773–8783.
Mumma M. J., Villanueva G. L., Novak R. E., Hewagama T., Bonev B. P., DiSanti M. A., Mandell A. M. and Smith M. D. (2009) Strong release of methane on mars in northern summer 2003. *Science* **323**, 1041–1045.
Nealson K. H., Inagaki F. and Takai K. (2005) Hydrogen-driven subsurface lithoautotrophic microbial ecosystems (SLiMEs): do they exist and why should we care? *Trends Microbiol.* **13**, 405–410.

O'Leary M. H. (1984) Measurement of the isotope fractionation associated with diffusion of carbon dioxide in aqueous solution. *J. Phys. Chem.* **88**, 823–825.

Oremland R. S., Marsh L. and DesMarais D. J. (1982) Methanogenesis in Big Soda Lake, Nevada: an alkaline, moderately hypersaline desert lake. *Appl. Environ. Microbiol.* **43**, 462–468.

Oremland R. S., Miller L. G. and Whiticar M. J. (1987) Sources and flux of natural gases from Mono Lake, California. *Geochim. Cosmochim. Acta* **51**, 2915–2929.

Oze C. (2005) Have olivine, will gas: serpentinization and the abiogenic production of methane on Mars. *Geophys. Res. Lett.* **32**. https://doi.org/10.1029/2005GL022691, [accessed February 7, 2014].

Penning H., Plugge C. M., Galand P. E. and Conrad R. (2005) Variation of carbon isotope fractionation in hydrogenotrophic methanogenic microbial cultures and environmental samples at different energy status. *Glob. Change Biol.* **11**, 2103–2113.

Pokrovsky O. S. and Schott J. (1999) Processes at the magnesium-bearing carbonates/solution interface. II. Kinetics and mechanism of magnesite dissolution. *Geochim. Cosmochim. Acta* **63**, 881–897.

Proskurowski G., Lilley M. D., Kelley D. S. and Olson E. J. (2006) Low temperature volatile production at the Lost City Hydrothermal Field, evidence from a hydrogen stable isotope geothermometer. *Chem. Geol.* **229**, 331–343.

Proskurowski G., Lilley M. D., Seewald J. S., Olson E. J., Früh-Green G. L., Lupton J. E., Sylva S. P. and Kelley D. S. (2008) Abiogenic hydrocarbon production at Lost City hydrothermal field. *Science* **319**, 604–607.

R Development Core Team (2008) *R: A Language and Environment for Statistical Computing*. R Foundation for Statistical Computing, Vienna Austria http://www.R-project.org.

Rempfert K. R., Miller H. M., Bompard N., Nothaft D., Matter J. M., Kelemen P., Fierer N. and Templeton A. S. (2017) Geological and geochemical controls on subsurface microbial life in the Samail Ophiolite, Oman. *Front. Microbiol.* **8**, [accessed March 13, 2017] http://www.ncbi.nlm.nih.gov/pmc/articles/PMC5293757/.

Robie R. A., Hemingway B. S. and Fisher J. R. (1978) *Thermodynamic Properties of Minerals and Related Substances at 298. 15 K and 1 Bar (10/Sup 5/ Pascals) Pressure and at Higher Temperatures*. Geological Survey, Washington, DC (USA), [accessed May 24, 2017] https://www.osti.gov/scitech/biblio/6877512.

Russell M. J., Hall A. J. and Martin W. (2010) Serpentinization as a source of energy at the origin of life: serpentinization and the emergence of life. *Geobiology* **8**, 355–371.

Sander R. (2015) Compilation of Henry's law constants (version 4.0) for water as solvent. *Atmos. Chem. Phys.* **15**, 4399–4981.

Scheller S., Goenrich M., Thauer R. K. and Jaun B. (2013) Methyl-coenzyme M reductase from methanogenic archaea: isotope effects on the formation and anaerobic oxidation of methane. *J. Am. Chem. Soc.* **135**, 14975–14984.

Schoell M. (1980) The hydrogen and carbon isotopic composition of methane from natural gases of various origins. *Geochim. Cosmochim. Acta* **44**, 649–661.

Sleep N. H., Meibom A., Fridriksson T., Coleman R. G. and Bird D. K. (2004) H2-rich fluids from serpentinization: geochemical and biotic implications. *Proc. Natl. Acad. Sci. USA* **101**, 12818–12823.

Suzuki S., Kuenen J. G., Schipper K., van der Velde S., Ishii S., Wu A., Sorokin D. Y., Tenney A., Meng X., Morrill P. L., Kamagata Y., Muyzer G. and Nealson K. H. (2014) Physiological and genomic features of highly alkaliphilic hydrogen-utilizing Betaproteobacteria from a continental serpentinizing site. *Nat. Commun.* **5**, [accessed November 19, 2014] http://www.nature.com/ncomms/2014/140521/ncomms4900/full/ncomms4900.html.

Szponar N., Brazelton W. J., Schrenk M. O., Bower D. M., Steele A. and Morrill P. L. (2013) Geochemistry of a continental site of serpentinization, the Tablelands Ophiolite, Gros Morne National Park: a Mars analogue. *Icarus* **224**, 286–296.

Takai K., Nakamura K., Toki T., Tsunogai U., Miyazaki M., Miyazaki J., Hirayama H., Nakagawa S., Nunoura T. and Horikoshi K. (2008) Cell proliferation at 122°C and isotopically heavy CH_4 production by a hyperthermophilic methanogen under high-pressure cultivation. *Proc. Natl. Acad. Sci.* **105**, 10949–10954.

Thauer R. K. (2011) Anaerobic oxidation of methane with sulfate: on the reversibility of the reactions that are catalyzed by enzymes also involved in methanogenesis from CO_2. *Curr. Opin. Microbiol.* **14**, 292–299.

Valentine D. L., Chidthaisong A., Rice A., Reeburgh W. S. and Tyler S. C. (2004) Carbon and hydrogen isotope fractionation by moderately thermophilic methanogens1. *Geochim. Cosmochim. Acta* **68**, 1571–1590.

Waite J. H., Combi M. R., Ip W.-H., Cravens T. E., McNutt R. L., Kasprzak W., Yelle R., Luhmann J., Niemann H., Gell D., Magee B., Fletcher G., Lunine J. and Tseng W.-L. (2006) Cassini ion and neutral mass spectrometer: enceladus plume composition and structure. *Science* **311**, 1419–1422.

Waite J. H., Glein C. R., Perryman R. S., Teolis B. D., Magee B. A., Miller G., Grimes J., Perry M. E., Miller K. E., Bouquet A., Lunine J. I., Brockwell T. and Bolton S. J. (2017) Cassini finds molecular hydrogen in the Enceladus plume: evidence for hydrothermal processes. *Science* **356**, 155–159.

Webster C. R., Mahaffy P. R., Atreya S. K., Flesch G. J., Mischna M. A., Meslin P.-Y., Farley K. A., Conrad P. G., Christensen L. E., Pavlov A. A., Martín-Torres J., Zorzano M.-P., McConnochie T. H., Owen T., Eigenbrode J. L., Glavin D. P., Steele A., Malespin C. A., Archer P. D., Sutter B., Coll P., Freissinet C., McKay C. P., Moores J. E., Schwenzer S. P., Bridges J. C., Navarro-Gonzalez R., Gellert R. and Lemmon M. T.Team the M. S. (2015) Mars methane detection and variability at Gale crater. *Science* **347**, 415–417.

Whiticar M. J. (1999) Carbon and hydrogen isotope systematics of bacterial formation and oxidation of methane. *Chem. Geol.* **161**, 291–314.

Worakit S., Boone D. R., Mah R. A., Abdel-Samie M.-E. and El-Halwagi M. M. (1986) Methanobacterium alcaliphilum sp. nov., an H2-utilizing methanogen that grows at high pH values. *Int. J. Syst. Bacteriol.* **36**, 380–382.

Woycheese K. M., Meyer-Dombard D. R., Cardace D., Argayosa A. M. and Arcilla C. A. (2015) Out of the dark: transitional subsurface-to-surface microbial diversity in a terrestrial serpentinizing seep (Manleluag, Pangasinan, the Philippines). *Front. Microbiol.* **6**, [accessed May 21, 2015] http://journal.frontiersin.org/Article/10.3389/fmicb.2015.00044/abstract.

Zyakun A. M. (1996) Potential of 13C/12C variations in bacterial methane in assessing origin of environmental methane. Available at: http://archives.datapages.com/data/specpubs/memoir66/25/0341.htm [Accessed December 15, 2016].

Associate editor: John W. Moreau